



DOI: 10.58224/2618-7183-2024-7-1-1



Field thermovision study of external enclosure for multi-storey residential building under climatic conditions of Northern Kazakhstan

Zhangabay N^{*1} , Giyasov A² , Ybray S³ , Tursunkululy T¹ , Kolesnikov A^{*1} 

¹ South-Kazakhstan University named after M. Auezov, Kazakhstan

² Moscow State University of Civil Engineering (MGSU), Russia,

³ Kazakh Agrotechnical Research University named after S. Seifullin, Kazakhstan.

Abstract. An in-place thermovision study was carried out in a multi-apartment apartment building of high comfort in a cold period of the year, located in the Northern part of the Republic of Kazakhstan in the work. The study result showed the presence of significant problems on thermal protection at the edge and inner corner fences where the temperature difference between the inner surface of an enclosure and the internal temperature was 6.4 - 19.4°C. An analysis of thermograms of window joints in living rooms also showed a significant temperature drop from -9.3°C to 18°C, where total vulnerable area was up to 10%. Thermograms of window-sill joints of living rooms also showed a temperature drop to -21.1 °C with an area of 15.7 %. The temperature on a reinforced concrete column's inner surface showed a value of 6.5 °C, which is typical for an area of 34.8 %. An analysis of outside and inside temperatures showed that as the temperature drops from -7 °C to -23 °C during the day, the inside temperature of the room remains relatively stable at 25.3 - 26.1 °C, although there are problems with the thermal protection of the enclosures, which indicates overconsumption of heat energy. Moreover, the internal air temperature exceeds the permissible temperature for living rooms by 1.3 - 2.6 °C. An analysis of air humidity also showed unsatisfactory values, which during the day varied from 17.4% to 21.2%. The deviations identified during the survey indicate the presence of problems on thermal protection of external enclosures, which require additional surveys aimed at further development and optimization of external enclosure designs to obtain optimal values in the issue of energy saving, considering the climatic characteristics of the Kazakhstan regions.

Keywords: thermovision study, cold period, residential building, external enclosure, thermal protection

Please cite this article as: Zhangabay N., Giyasov A., Ybray S., Tursunkululy T., Kolesnikov A. Field thermovision study of external enclosure for multi-storey residential building under climatic conditions of Northern Kazakhstan. *Construction Materials and Products*. 2024. 7 (1). 1. DOI: 10.58224/2618-7183-2024-7-1-1

*Corresponding author E-mail: kas164@yandex.kz

1. INTRODUCTION

Energy saving in construction has been studied practically all over the world and for quite a long time. It is evident that this problem with the introduction of energy-efficient new structural solutions, construction and thermal insulation materials, as well as adoption of appropriate programs and strategies becomes more and more relevant every year, as buildings consume about 30% of all energy in the world [1,2]. To address this problem on an international scale, various strategies to modernize residential buildings to improve their energy efficiency were developed in many countries of the European Union [3, 4, 5]. Numerous studies are devoted to solving this problem, the results of which are used in development of various programs at both local and state levels [6, 7, 8, 9]. In this case, a correct choice of the design of external enclosure contributes to a significant reduction of heat energy consumption.

In the Republic of Kazakhstan, heat consumption to serve the residential buildings is more than 40% of the total energy consumed [10]. A significant part of consumption falls on the share of multi-apartment residential buildings, the consumption of which represents more than 70% of total housing sector [11], equivalent to 80,000 houses, of which 18,000 require major repairs. These indicators demonstrate an importance of the state policy and adoption of appropriate programs to improve the issue of energy saving in buildings under construction and existing buildings [12, 13, 14, 15, 16, 17]. In this connection, the design of external enclosures is the most important task in reducing heat energy costs, a correct choice of which can contribute to increasing the energy efficiency of buildings by almost 3 times [18, 19, 20, 21, 22]. But to achieve such results it is necessary to assess the issue of thermal protection of enclosures correctly, which is carried out by non-destructive testing method [23, 24, 25, 26, 27]. Currently there are practically no data in scientific and technical literature in the Republic of Kazakhstan on thermovision monitoring of multi-apartment residential buildings with quantitative-qualitative impact assessment of thermal energy loss through external enclosures, which requires additional research in this area. Considering these circumstances, at the initial stage of an integrated study, the objective of this work is an in-place thermovision study of a residential building in the coldest period of the year, located in the northern part of the Republic, where the main task is to identify vulnerable areas in the external enclosure, which significantly affect the thermal energy consumption. As a result of which in the future new energy-efficient designs of external enclosures will be developed and scientifically substantiated, considering climatic peculiarities of the Republic of Kazakhstan territories.

2. METHODS AND MATERIALS

2.1 Thermovision survey method

Field studies of external enclosure of a multi-storey residential building in order to identify vulnerable areas with disturbed thermal protection properties was carried out according to the method of thermovision study (GOST Z 54852). Devices specified in Table 1, complying with the standard, verified according to the standard, were used in the study (GOST R 8.619).

Table 1. Name and characteristics of the devices.

No.	Device	Charateristics
1	Thermal imager testo 875-2i	Low temperature version (measurement from -30 °C, display from -50 °C) High temperature measurement up to 550°C
2	Thermal hygrometer Xiaomi	Temperature and humidity sensor with measuring range: temperature 0°C ~ 60 °C; humidity 0~99,6 %
3	Pyrometer (no-contact thermometer) RZ GM380	Measurement range -50 ~380 °C
4	Laser rangefinder ELITECH ЛД 80Prof	Calculation of area and volume of the premises, height measurement with adjacent measurements, and slope measurements to ±90 °.
5	Mechanical tape measure	Metal, measuring range up to 10m
6	Digital camera Sony ILCE-6400L	The camera is equipped with a 24.2 MP APS-C format Exmor™ CMOS matrix

2.2 Object of thermovision study

Ten-storey residential building with increased comfort from reinforced concrete frame design solution with ventilated facade, located in Astana, the Republic of Kazakhstan, the layout diagram of which is presented in Fig. 1, was considered as an object of research.

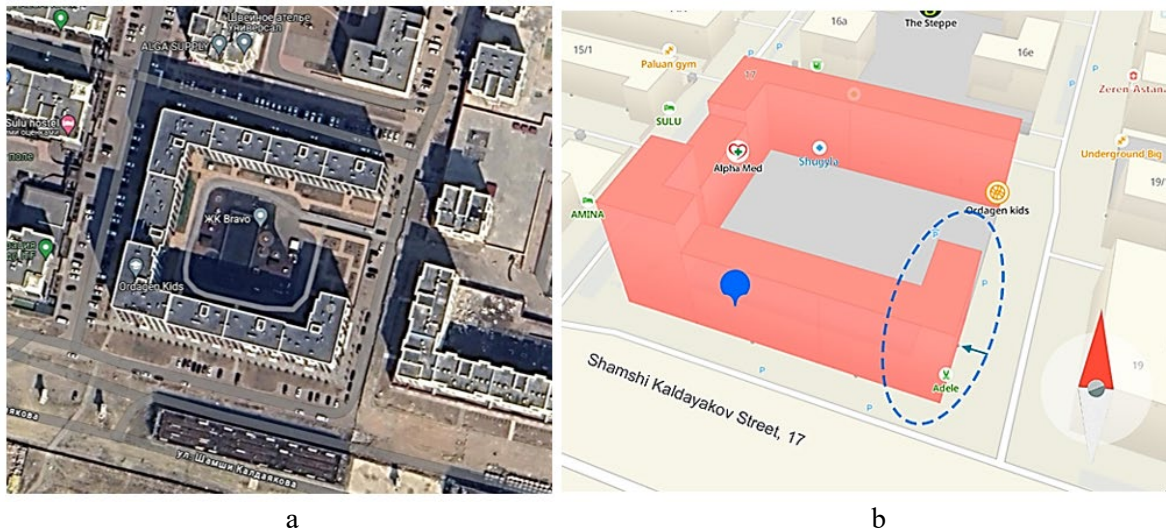


Fig. 1. Layout diagram of a research object: a- aerial view, b-side view.

The eastern side of “Bravo” residential complex, located on Sh. Kaldayakov Street, Astana, was chosen as an orientation of the study, which is located on the parallel 51°6’58’’ N and 71°28’40’’ E, which belongs to the I-B climatic zone (SP RK 2.04-01-2017).

The general in-place of the building with structural facade cladding is shown in Fig. 2 a, the main design solution of external enclosure with geometric and thermal insulation parameters is shown in Fig. 2 b and in Table 2.



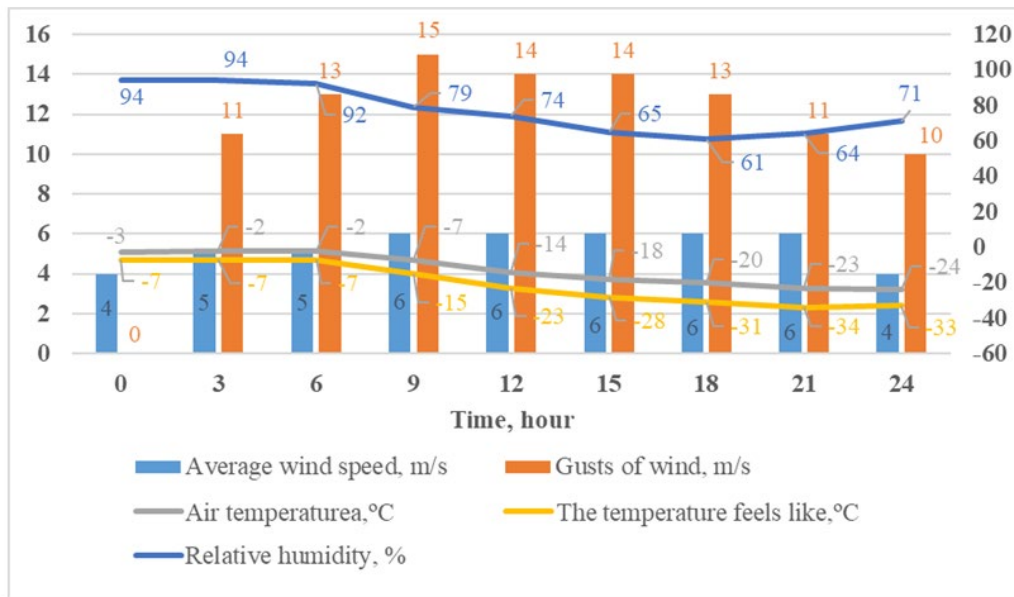
Fig. 2. Object facade: a– in-place facade; b- design solution of external enclosure.

Table 2. Geometric parameters and thermal insulation properties of the layers of external enclosure in accordance with Figure 2b.

Number of layer	Type of layer material	Thickness of layer, mm	Layer thermal conductivity coefficient, λ , (W/(m·°C))	Layer heat absorption, S, (W/(m·°C))	Layer vapor permeability, μ , (mg/m·h·Pa)
1	Cladding layer of aluminum composite panels	4	–	–	–
2	Air interlayer	150	–	–	–
3	Mineral wool board insulation with density of 150 kg/m^3	100	0.037	0.68	0.31
4	Foam block masonry with a density of $(30 \times 30 \times 60) 800 \text{ kg/m}^3$	300	0.210	4.92	0.14
5	Complex solution of density 1800 kg/m^3	15	0.760	9.6	0.09

2.3 Climatic conditions as of the date of the study

The coldest winter period (SP RK 2.04-01-2017) was chosen as the date of the study, and the thermovision study itself was conducted on 14.01.2024. The main climatic indicators at the date of the study are presented in Fig. 3

**Fig. 3.** Main climatic indicators on 14.01.2024.

3. RESULTS AND DISCUSSIONS

3.1. Thermal characteristics of residential building enclosures

3.1.1 External wall construction

In accordance with the design solutions presented (Fig. 2b and Table 2), a thermal calculation of an external wall of the multistory residential complex of high comfort was carried out. Initially, the actual design heat transmission resistance (R) was determined and compared with a required one (R_i) based on the heating season degree-day (HSDD) by SP RK 2.04-107-2022, the calculation results are presented in the table below 3.

$$R_f = \frac{1}{\alpha_1} + \frac{\delta_1}{\lambda_1} + \frac{\delta_2}{\lambda_2} + \frac{\delta_3}{\lambda_3} + \frac{1}{\alpha_2}, \quad (1)$$

$\delta_{1,2,3}$ – thickness of layer, mm

λ – layer heat conductivity coefficient, W/m · °C

λ_1 and λ_2 – heat transmission coefficients of external and internal surfaces, W/m² · °C

The required design resistance (R_t) was determined by expression (2), Table 3

$$HSDD=(t_1+t_2) \cdot Z = 6170 \text{ }^\circ\text{C}/24 \text{ hours}, \quad (2)$$

t_1 – design temperature of indoor air, °C (GOST 30494)

t_2 – average temperature, °C (BCaR 2.01.01-82)

Z – duration of a period with average daily air temperature below or equal to 8°C, day (BCaR 2.01.01-82).

Table 3. Calculation results of the design heat transmission resistance.

Number of layer	Type of layer material	Thickness of layer, mm	Layer thermal conductivity coefficient, λ , (W/(m·°C))	Calculated heat transmission resistance of a layer, R, (m ² . °C/W)
λ_1	–	–	–	0.04
1	Complex solution of density 1800 kg/m ³	15	0.760	0.02
2	Foam block masonry with a density of 800 kg/m ³	300	0.210	1.43
3	Mineral wool board insulation with density of 150 kg/m ³	100	0.037	2.70
λ_2	–	–	–	0.11
R_f				4.31
R_t				3.56

Based on the design solution, the thermal calculation of external wall is in accordance with requirement $R_f > R_t$ (SP RK 2.04-107-2022). The value of the cladding layer and ventilated layer on enclosure design resistance was not considered in the calculation, as the temperature in the ventilated layer in winter is the same as the ambient temperature (SP RK 2.04-107-2022).

3.1.2. Construction of a translucent window area

Construction of a translucent window aperture is equal to 2400×1700mm with insulated glass unit made of ordinary glass with 12 mm glass spacing and hard selective coating, Fig.4.



Fig. 4. Translucent window aperture: a – view of a in-place window; b – name of the translucent window aperture construction: 1-air chamber, 2-glass sheet, 3-distance frame, 4-molecular sieve, 5-sealant.

A translucent construction was selected as per norm SP RK 2.04-107-2022, where in accordance with a calculation method the heat transfer resistance R_s of translucent constructions is determined on the basis of SN RK 2.04.04-2011. Here, first of all, the heating season degree-days (HSDD) indicator was calculated and the value R_s was determined based on it, and the design selection was carried out by value of the reduced heat transmission resistance R_d . Thus, the design of a translucent aperture chosen at the design stage meets the condition $R_d \geq R_s$.

3.1.3 Construction of the upper floor slab

When inspecting the upper floor, it was found that the slab consists of three layers, where the first layer is a reinforced concrete slab with a thickness of 220mm, the second layer is an air layer with a thickness of 1500mm, which performs the function of confinement in winter, having a positive effect on the design resistance in general. In summer, when special glazed openings are opened, the air layer serves as a ventilated layer, which also has a positive effect on the thermal qualities and prevents the attic space from overheating. Reinforced concrete roofing with a thickness of 220mm is also provided as the last layer. This design of the floor is characteristic for a roof with a warm attic, where a feature of the design solution is that air from the ventilation units of the underlying floors enters the attic space, and then goes into the atmosphere through the attic exhaust shaft, which is usually arranged one for each section of the building. Thus, the entire volume of the attic, heated by warm ventilation air from the premises, is a prefabricated static pressure ventilation chamber that is connected to the ventilation system of a residential building. In this case, the air temperature drop in the warm attic space below $+12^\circ\text{C}$ is not allowed SP RK 2.04-107-2022.

3.2 Thermovision study of external enclosure of a residential building

Thermovision study of external enclosures in a continuous exterior section, window aperture, upper floor slabs was done during a day with recording the temperature and humidity values in the morning (9:00 - 10:00), in the middle of the day (14:00 - 15:00) and at night (21:00 - 22:00), where the values of outdoor temperature are shown in Fig. 3, and the premises microclimate is shown in Table 4.

Table 4. Values of premises microclimate indicators at the time of survey.

No.	Survey time, h	Indoor air temperature, °C	Indoor air humidity, %
1	9:00 – 10:00	25.3	17.4
2	14:00 – 15:00	25.8	21.2
3	21:00 – 22:00	26.1	19.3

The study object was a 3-room apartment on the fifth floor with a total area of 93 m^2 (items 3.2.1 and 3.2.2) with a room height of 3 m and a similar apartment on the tenth floor above, where the main objective of study was the floor slabs of the tenth floor above it этажа (p. 3.2.3), Fig. 5.

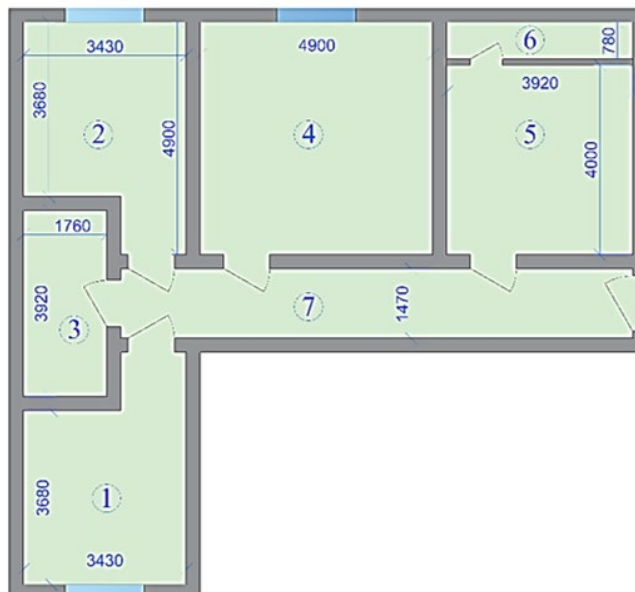


Fig. 5. Plan of the apartment studied on the fifth floor: 1 – north-oriented bedroom (No.1); 2 – south-oriented bedroom (No.2); 3 – bathroom; 4 – hall; 5 – kitchen; 6 – balcony.

3.2.1 Study of continuous external enclosure and corner joints

Fig. 6-11 show thermograms and analysis of outdoor temperature impact on thermal conductivity of upper corner joints (left and right) of room No.1 at different times of the day as per Table 4.

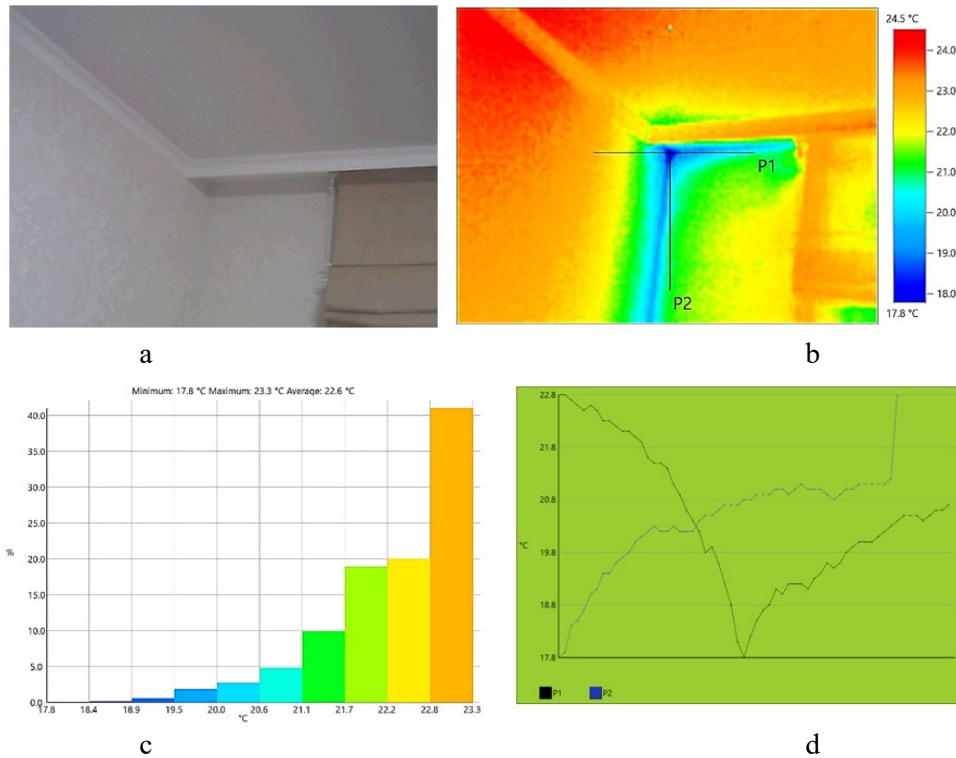


Fig. 6. A thermogram of the left upper vertical corner joint of room No.1 between 9:00 and 10:00h: a – in-place photo; b – thermogram; c – diagram of the area covered by the respective temperature; d – diagram of horizontal (P1) and vertical (P2) temperature values relative to Fig. b.

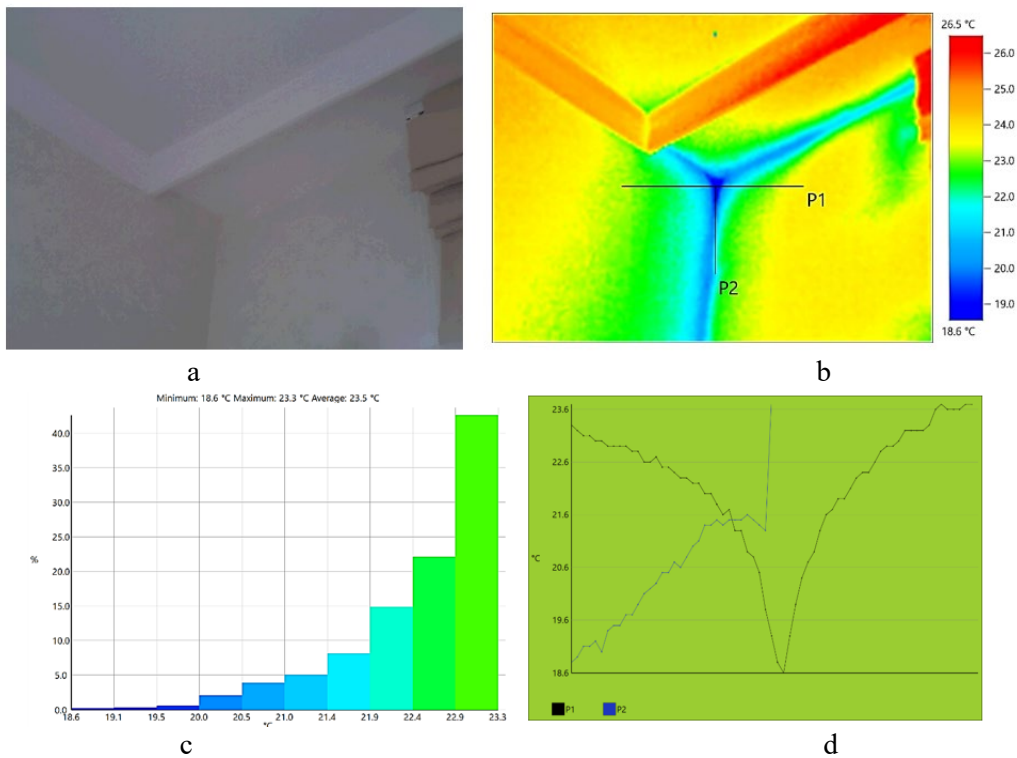


Fig. 7. A thermogram of the left upper vertical corner joint of room No.1 between 14:00 and 15:00h: a – in-place photo; b – thermogram; c – diagram of the area covered by the respective temperature; d – diagram of horizontal (P1) and vertical (P2) temperature values relative to Fig. b.

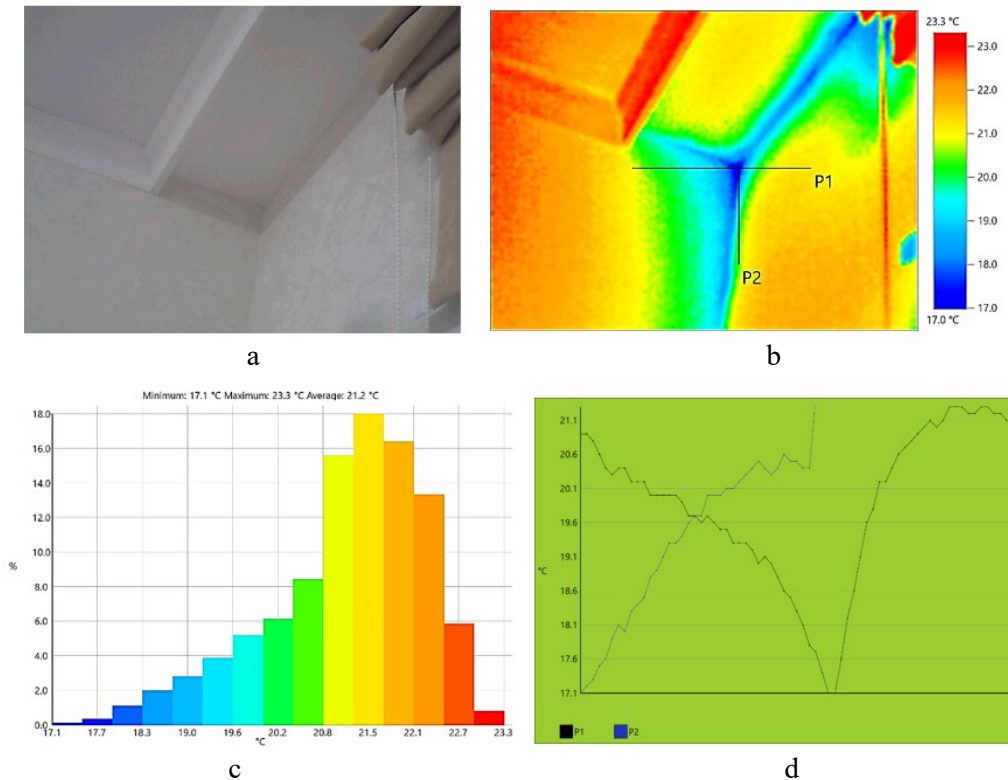


Fig. 8. A thermogram of the left upper vertical corner joint of room No.1 between 21:00 and 22:00h: a – in-place photo; b – thermogram; c – diagram of the area covered by the respective temperature; d – diagram of horizontal (P1) and vertical (P2) temperature values relative to Fig. b.

During survey period the temperature and humidity of the external environment in accordance with Figure 3 (a) is equal to: in the morning (9:00 - 10:00) $t = -7^{\circ}\text{C}$ and $\varphi = 79\%$, in the lunchtime (14:00 - 15:00) $t = -16^{\circ}\text{C}$ and $\varphi = 70\%$, and at night (21:00 - 22:00) $t = -23^{\circ}\text{C}$ and $\varphi = 64\%$. Indoor microclimate indicators are presented in Table 4.

An analysis of the thermograms in the upper left corner on Figures 6-8 shows that the temperature difference between the enclosure surface temperature and the internal air temperature was $7.2 - 9.0^{\circ}\text{C}$ dependent on the survey time (Table 4). Furthermore, the enclosure surface temperature shows a positive value of $17.1 - 18.6^{\circ}\text{C}$ due to an increase of heater output, which leads to excessive overconsumption of heat energy, as well as an increase of internal room temperature (Table 4), which is contrary to the standard GOST 30494. At that, if heater output is reduced, the internal surface temperature of external enclosure will decrease, that indicates insufficient thermal protection of the enclosure in the survey area, Fig. 6 – 8. Besides, the indoor humidity indicated in Table 4 in all cases of the survey shows a lower than optimal value, which also contradicts the specified standard GOST 30494.

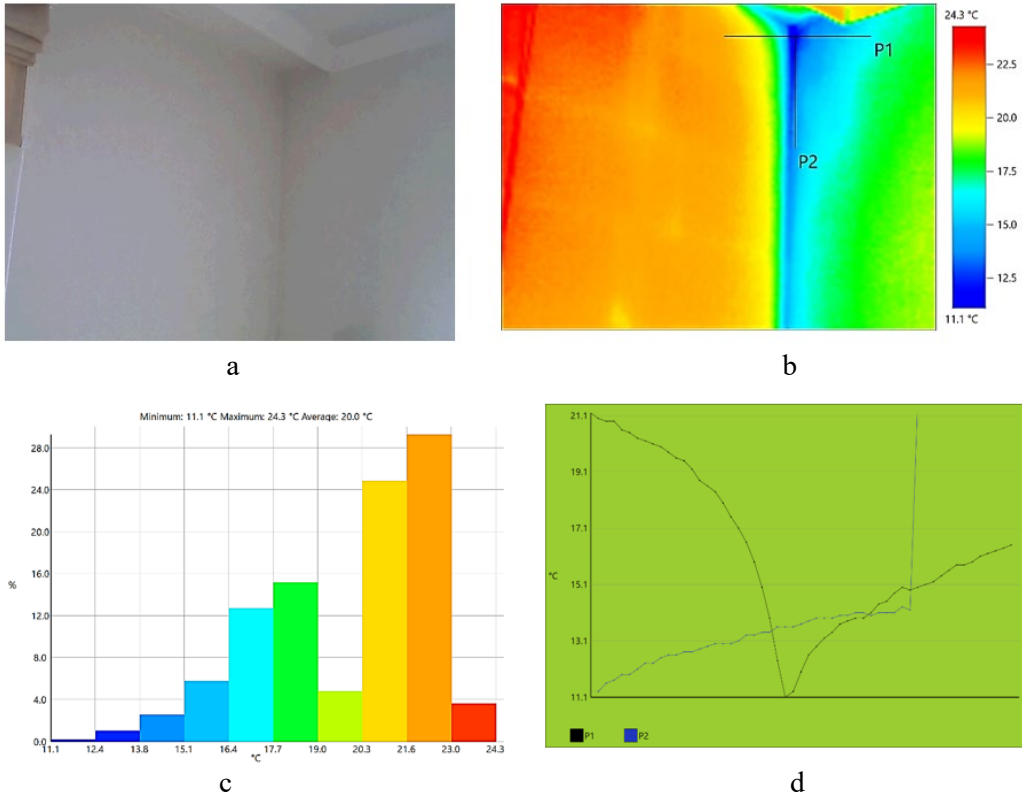


Fig. 9. A thermogram of the right upper vertical corner joint of room No.1 between 09:00 and 10:00h: a – in-place photo; b – thermogram; c – diagram of the area covered by the respective temperature; d – diagram of horizontal (P1) and vertical (P2) temperature values relative to Fig. b.

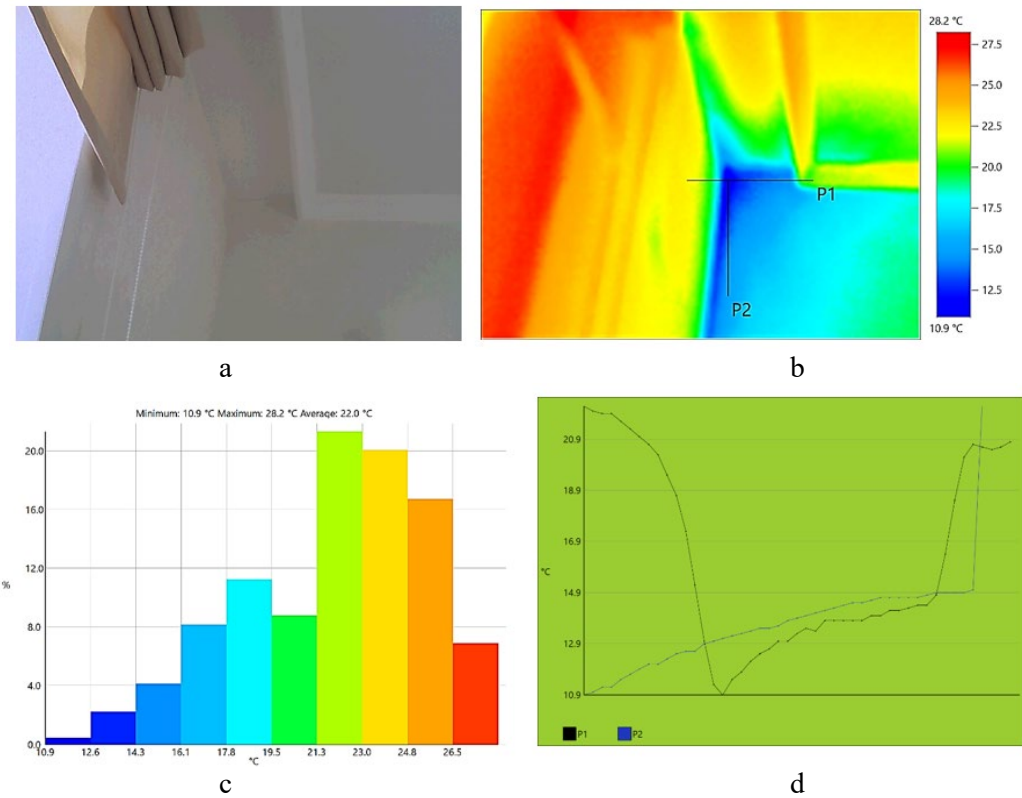


Fig. 10. A thermogram of the right upper vertical corner joint of room No.1 between 14:00 and 15:00h: a – in-place photo; b – thermogram; c – diagram of the area covered by the respective temperature; d – diagram of horizontal (P1) and vertical (P2) temperature values relative to Fig. b.

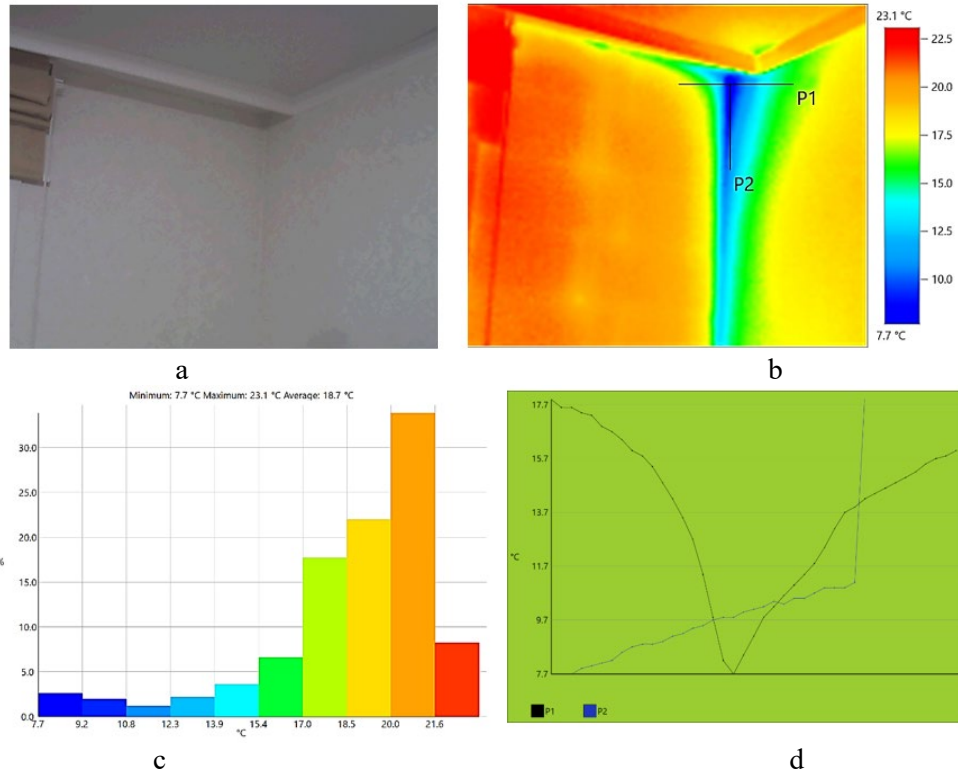


Fig. 11. A thermogram of the right upper vertical corner joint of room No.1 between 21:00 and 22:00h: a – in-place photo; b – thermogram; c – diagram of the area covered by the respective temperature; d – diagram of horizontal (P1) and vertical (P2) temperature values relative to Fig. b.

An analysis of the thermograms in the right left corner of a room No.1 showed (Figure 9-11) that thermal protection relatively to the considered left corner (Figure 6-8) turned out to be significantly lower. Thus, the temperature drop between the internal surface of external enclosure and the internal air temperature was 14.2 - 18.4 °C (Figure 9-11), which also fails to meet the requirements SP RK 2.04-107-2022 and indicates a problem of thermal energy overconsumption at the cost of maintaining the required indoor temperature. But excessive increase of heater outputs leads to the issue of indoor overheating (Table 4), but it does not resolve the issue of thermal protection of external enclosure.

The thermograms and analysis of the outdoor temperature impact on the thermal protections at the upper corner joints (left and right) of Room No.2 at different times of the day are shown in Fig. 12-17 as per Table 4.

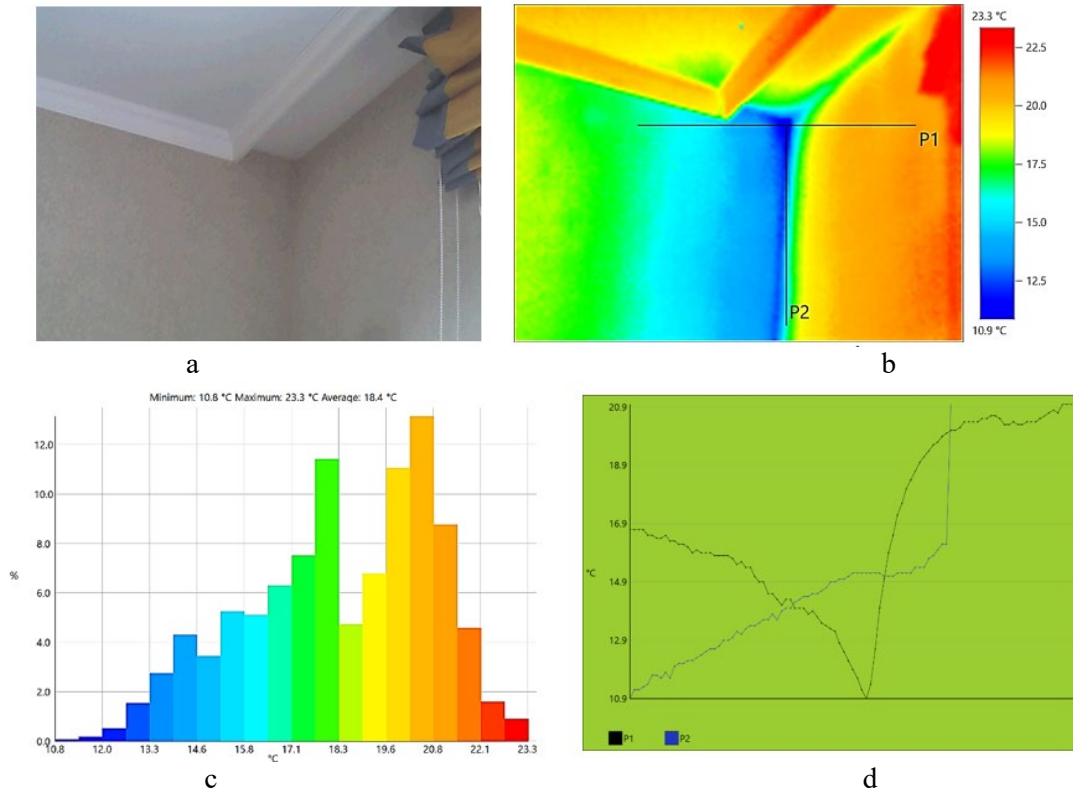


Fig. 12. A thermogram of the left upper vertical corner joint of room No.2 between 9:00 and 10:00h: a – in-place photo; b – thermogram; c – diagram of the area covered by the respective temperature; d – diagram of horizontal (P1) and vertical (P2) temperature values relative to Fig. b.

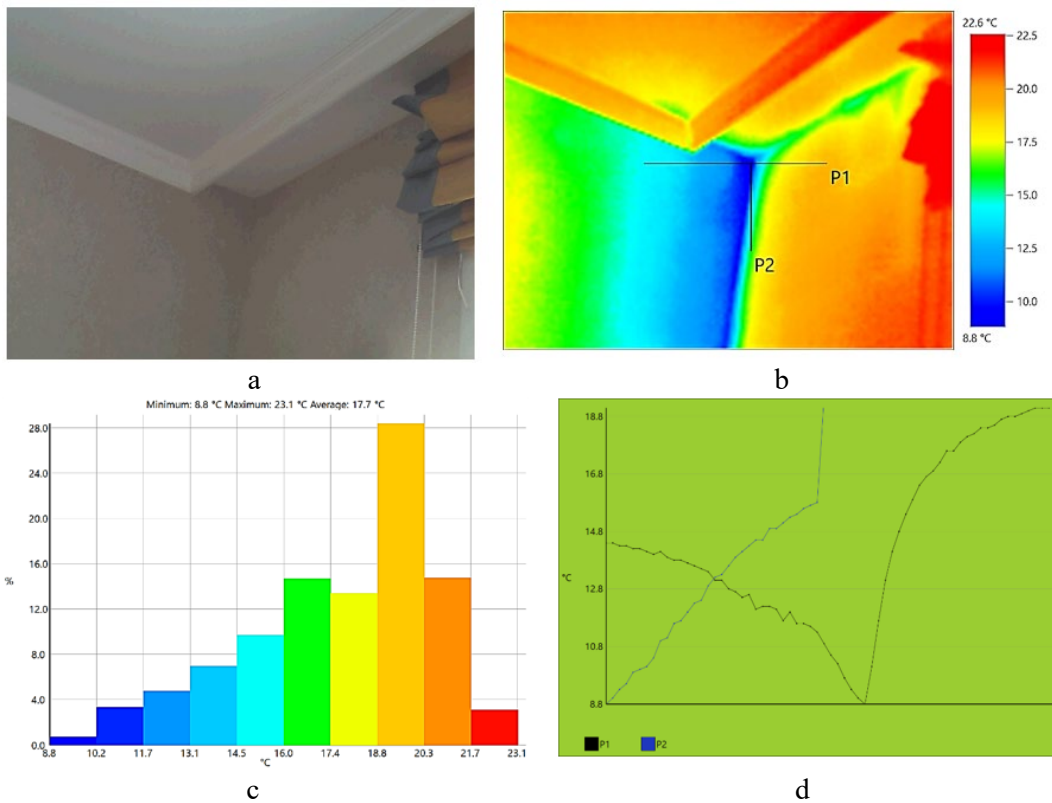


Fig. 13. A thermogram of the left upper vertical corner joint of room No.2 between 14:00 and 15:00h: a – in-place photo; b – thermogram; c – diagram of the area covered by the respective temperature; d – diagram of horizontal (P1) and vertical (P2) temperature values relative to Fig. b

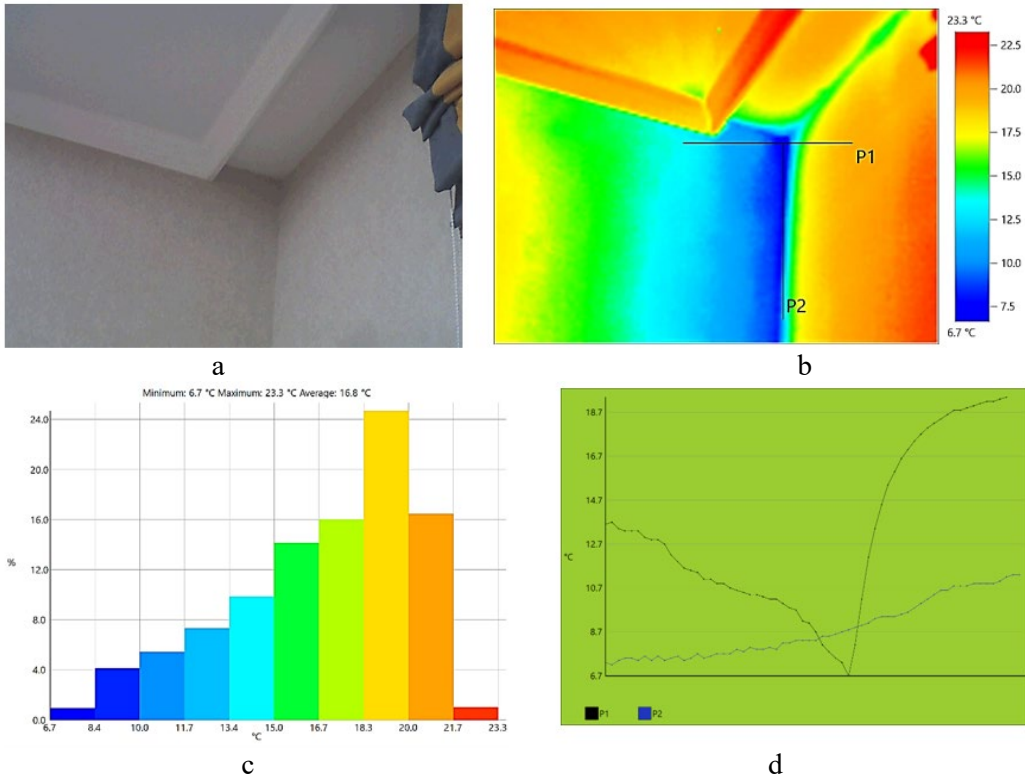


Fig. 14. A thermogram of the left upper vertical corner joint of room No.2 between 21:00 and 22:00h: a – in-place photo; b – thermogram; c – diagram of the area covered by the respective temperature; d – diagram of horizontal (P1) and vertical (P2) temperature values relative to Fig. b.

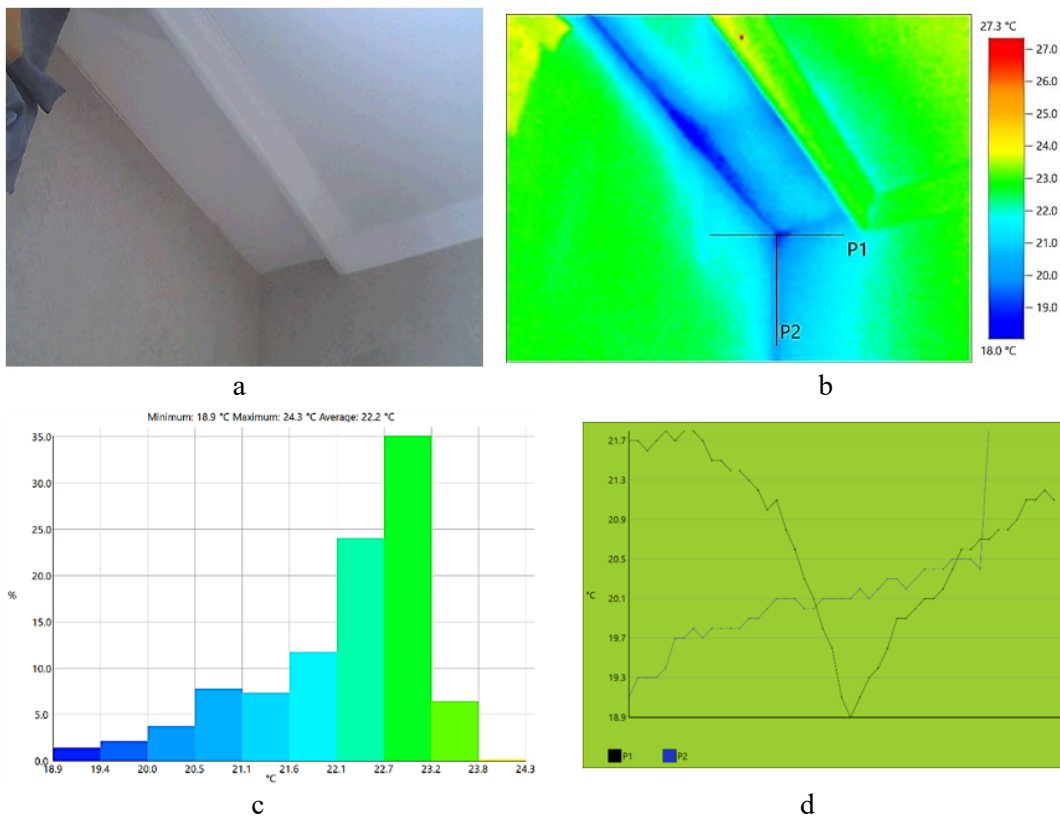


Fig. 15. A thermogram of the right upper vertical corner joint of room No.2 between 9:00 and 10:00h: a – in-place photo; b – thermogram; c – diagram of the area covered by the respective temperature; d – diagram of horizontal (P1) and vertical (P2) temperature values relative to Fig. b.

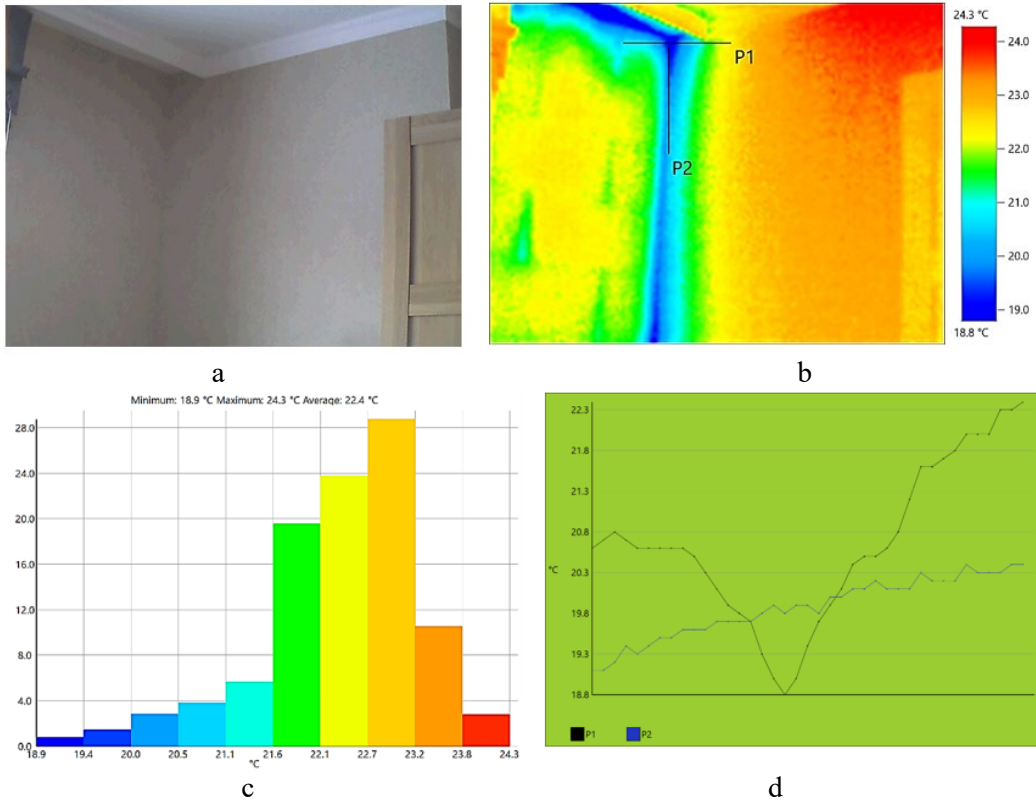


Fig. 16. A thermogram of the right upper vertical corner joint of room No.2 between 14:00 and 15:00h: a – in-place photo; b – thermogram; c – diagram of the area covered by the respective temperature; d – diagram of horizontal (P1) and vertical (P2) temperature values relative to Fig. b.

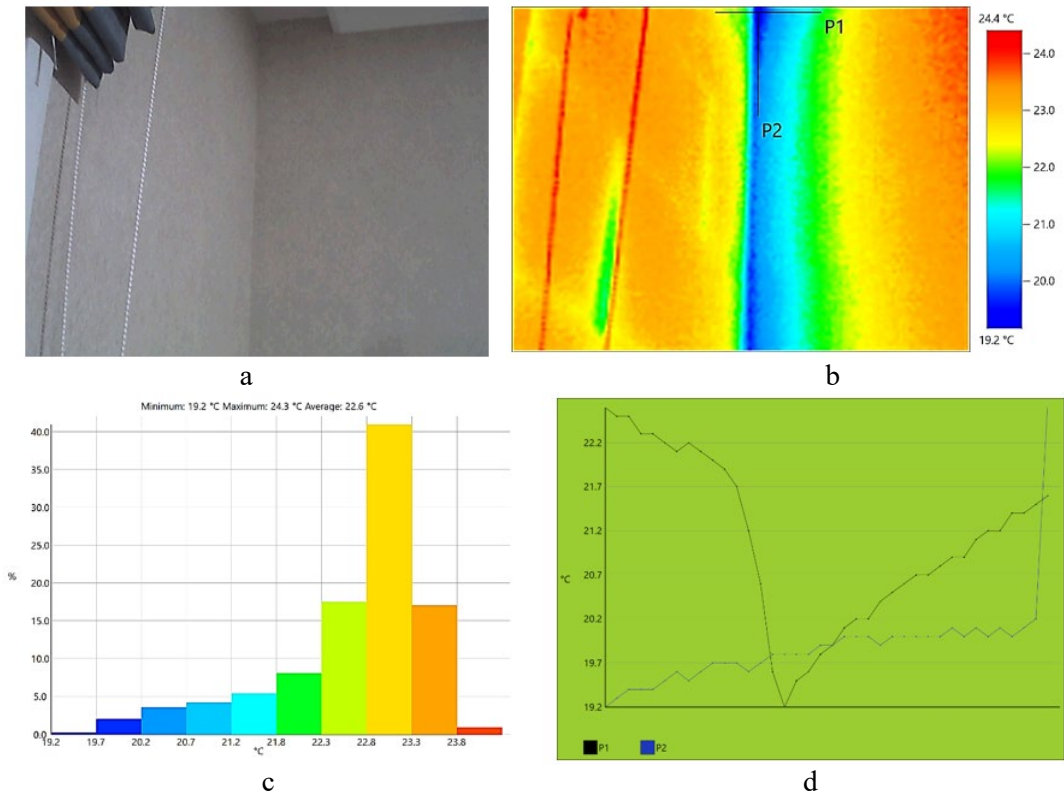


Fig. 17. A thermogram of the right upper vertical corner joint of room No.2 between 21:00 and 22:00h: a – in-place photo; b – thermogram; c – diagram of the area covered by the respective temperature; d – diagram of horizontal (P1) and vertical (P2) temperature values relative to Fig. b.

Thermograms of the left vertical corner joint in Room No.2 indicate an excessive temperature drop between internal enclosure surface and internal air temperature, where the value of drop was 14.5 - 19.4 °C. (Fig. 12-14), this indicates non-compliance with the standard SP RK 2.04-107-2022, the implications of which influence excessive thermal energy consumption to maintain appropriate temperature (Table 4). An analysis of the right vertical corner joint in this room showed a slight deviation, which is equal to an average of 6.4 %, Fig. 15-17.

3.2.2 Study of vulnerabilities that affect heat losses in the residential premises

An analysis of sub-section 3.2.1 showed that the most maximum heat losses occur during the night time between 21:00 and 22:00 h, therefore further study of vulnerabilities for a more accurate analysis was performed at these times, Fig. 18-22

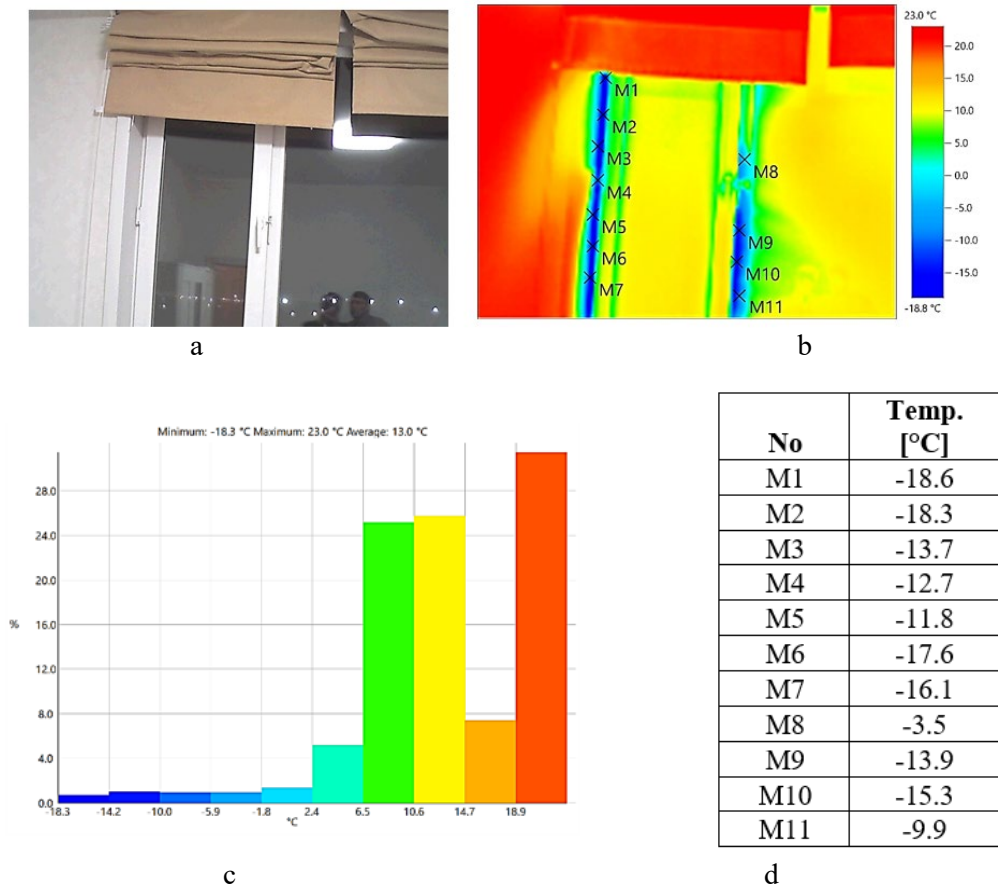


Fig. 18. A thermogram of the left vertical joint of external window in room No.1: a – in-place photo; b – thermogram with characteristic points; c – diagram of the area covered by the respective temperature; d – table of point values on the enclosure of Fig. b.

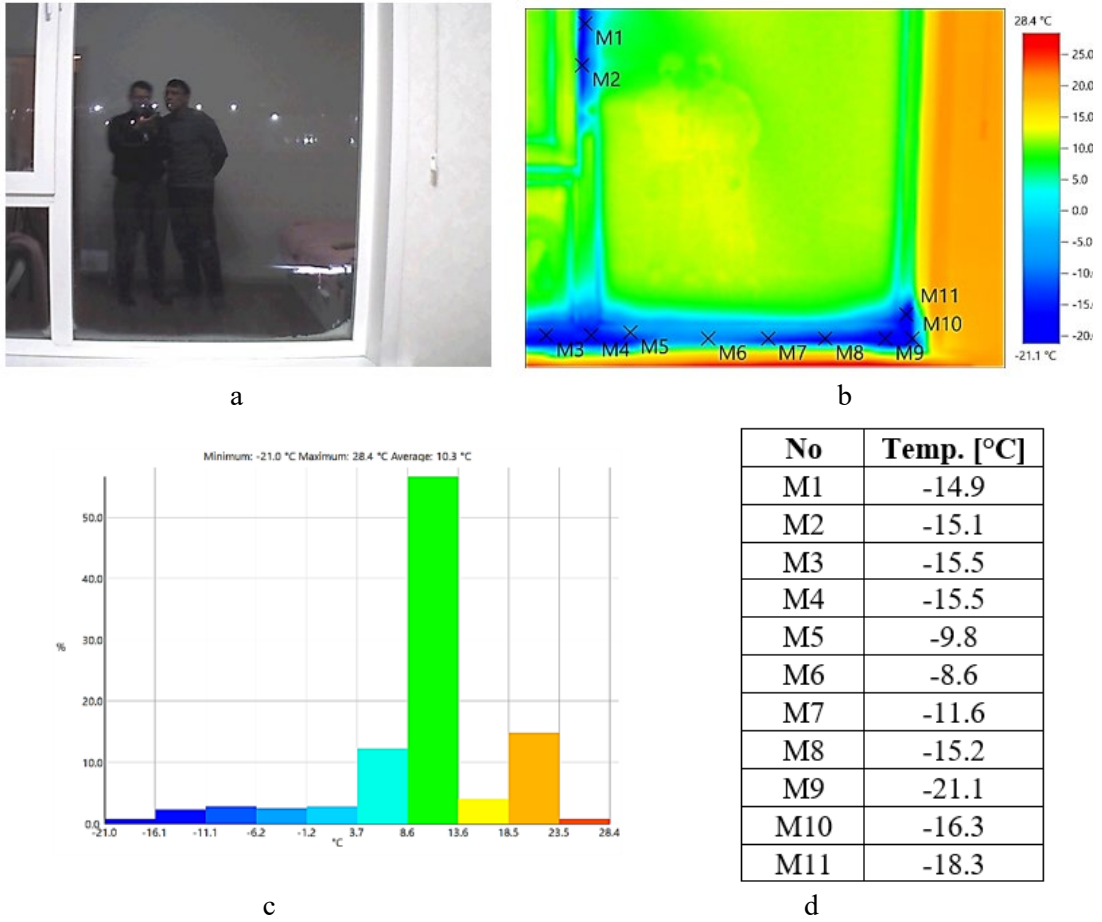
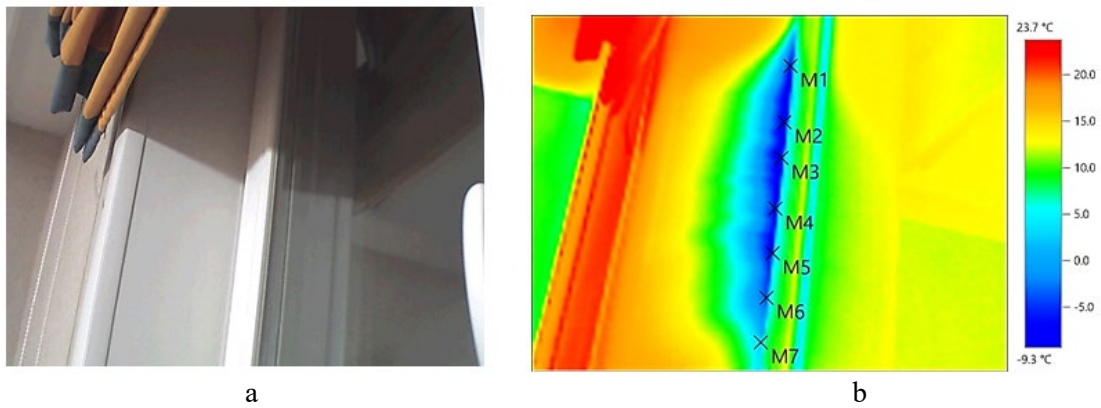
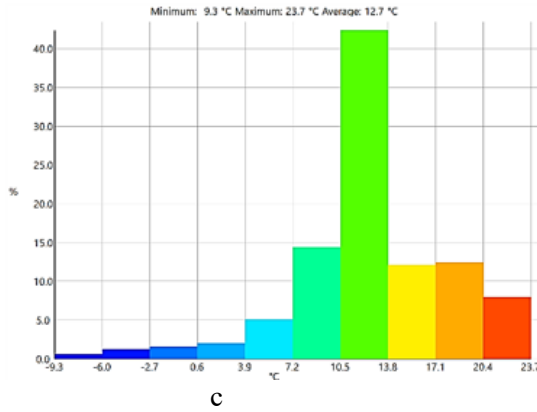


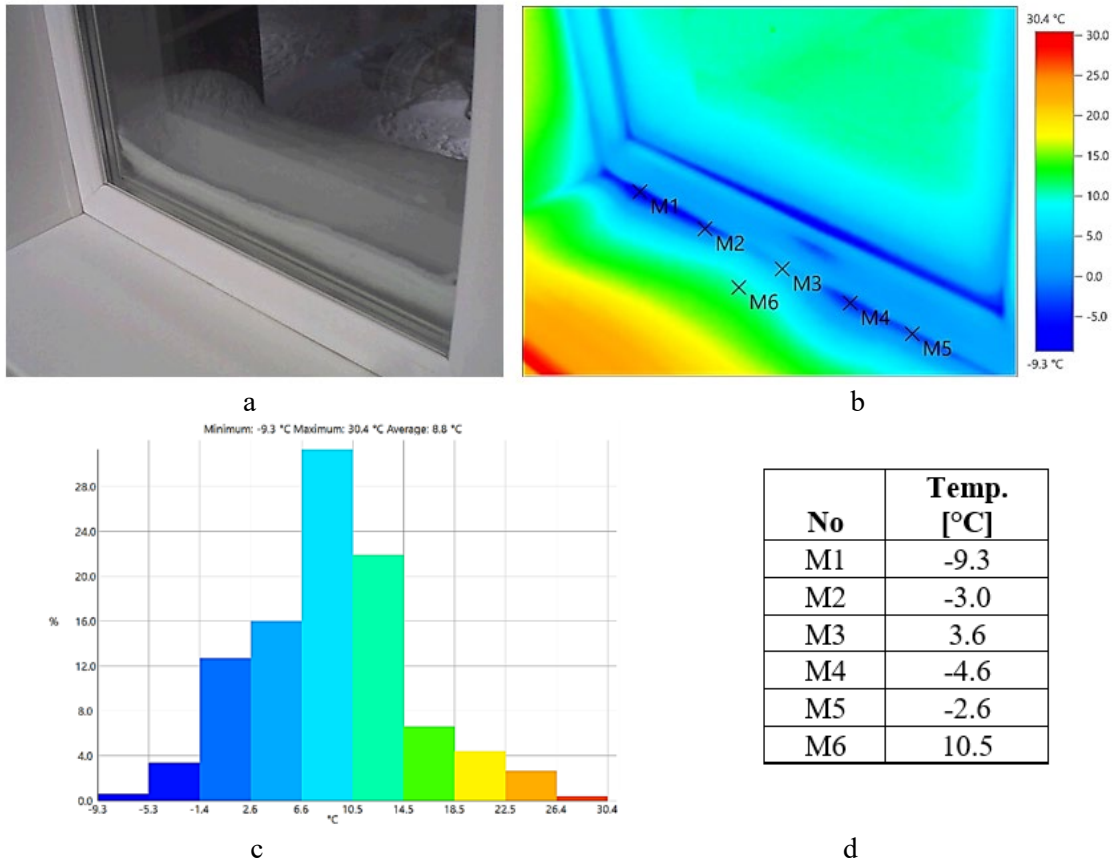
Fig. 19. A thermogram of the windowsill of external window in room No.1: a – in-place photo; b – thermogram with characteristic points; c – diagram of the area covered by the respective temperature; d – table of point values on the enclosure of Fig. b.





No	Temp. [°C]
M1	-5.7
M2	-8.2
M3	-9.3
M4	-6.9
M5	-5.0
M6	-3.8
M7	2.2

Fig. 20. A thermogram of the left vertical joint of external window in room No.2: a – in-place photo; b – thermogram with characteristic points; c – diagram of the area covered by the respective temperature; d – table of point values on the enclosure of Fig. b.



No	Temp. [°C]
M1	-9.3
M2	-3.0
M3	3.6
M4	-4.6
M5	-2.6
M6	10.5

Fig. 21. A thermogram of the windowsill of external window in room No.2: a – in-place photo; b – thermogram with characteristic points; c – diagram of the area covered by the respective temperature; d – table of point values on the enclosure of Fig. b.

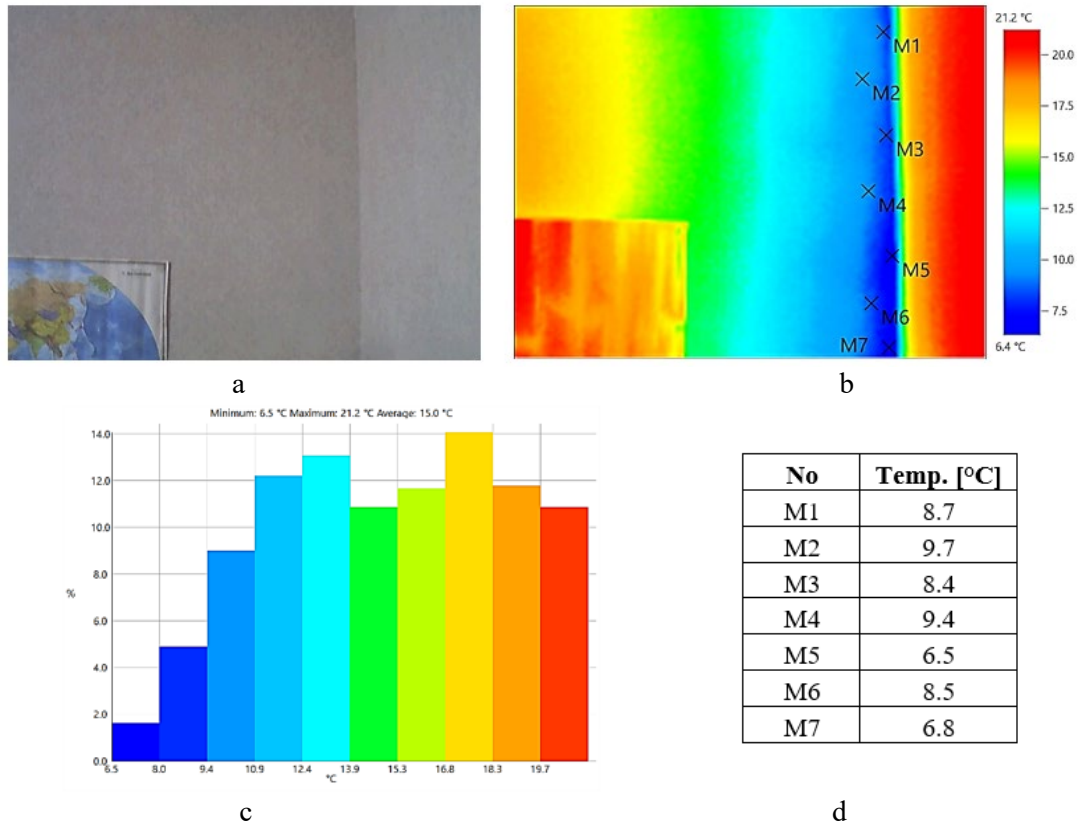


Fig. 22. A thermogram of the reinforced concrete column in room No.2: a – in-place photo; b – thermogram with characteristic points; c – diagram of the area covered by the respective temperature; d – table of point values on the enclosure of Fig. b.

Based on thermovision survey of vulnerable places in residential premises (Fig. 18-22) it was determined that the left vertical joint of external window in room No.1 (Fig.18a) does not comply with the standards SP RK 2.04-107-2022, as temperature at the external wall and frame of the translucent aperture showed a significant temperature drop (Fig.18 d) with maximum temperature of -18 °C at the point M1 (Figure 17 b). All in all, the zone of unfavorable temperature of the vertical opening considered (Fig.17 a) is 10% (Fig. 18 c) of the total area of Fig. 18 (a, b). Survey of the window sill in this room showed (Figure 19 a) that it also does not comply with the thermal protection standards SP RK 2.04-107-2022. As there is a significant temperature drop (Fig.19 d), where minimum temperature on the window sill was -21.1 °C, which is typical to point M9 (Fig. 19 b). The zone of unfavorable of window sill temperature is 15.7% (Figure 19 c) of the total area, Survey of the window sill in this room showed (Fig. 19 a) that it also does not comply with the thermal protection standards. As there is a significant temperature drop (Fig.19 d), where minimum temperature on the window sill was -21.1 °C, which is typical to point M9 (Fig. 19 b). The zone of unfavorable of window sill temperature is 15.7% (Fig. 19 c) of the total area, Fig. 19 (a, b).

A similar problem with vulnerable locations was also detected in Room No.2 (Fig. 20 a). As per Fig. 20 (b) the minimum surface temperature at the left opening joint is -9.3 °C (Fig. 20 d), which is characteristic to point M3, and the total area of unfavorable temperature is 10.1 % (Fig. 20 c) of the total area of Fig. 20 (a, b). Survey of the window sill in this room also showed inadequate thermal protection (Fig.21a). The lowest temperature measured by the thermogram isotherm (Fig. 21 b) is equal to -9.3 °C, which is characteristic to point M1, where the unfavorable window sill area is 6.9 % of the total area of Fig. 21 (a, b). Study of the left external corner (Fig. 22a), where the reinforced concrete column is located, also shows the existence of a thermal protection problem. The isotherms on the thermogram of Figure 22 (b) on the surface of minimum temperature is equal to 6.5 °C, which is characteristic to point M5. The unfavorable area was 34.8 % of the total, Fig. 22 (a, b), which also does not meet the standard on thermal protection of buildings SP RK 2.04-107-2022.

3.2.3 Survey of compliance between translucent openings and upper floor slab

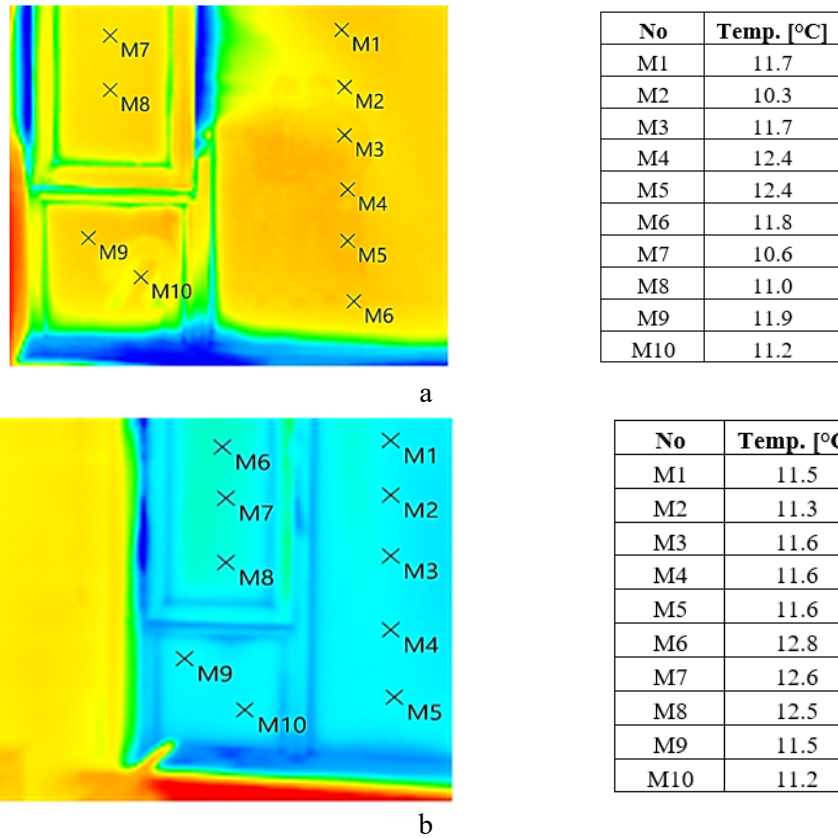


Fig. 23. Thermogram of the surface in the translucent aperture: a – room No.1; b – room No.2.

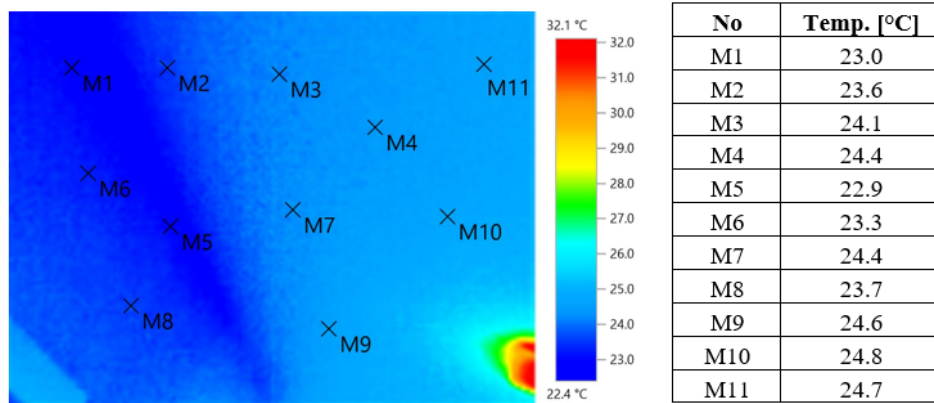


Fig. 24. Thermogram on internal surface of the upper floor slab.

Survey of the translucent enclosure surface in the premises indicates that the design layout of a translucent enclosure, discussed in subsection 3.1.2 is accepted correctly. As, in accordance with the thermogram of Fig. 23 the average temperature of isotherm, Fig.23 (a) was 11.5 °C, and on the surface, Fig. 23 (b) the value of isotherm was 11.8 °C, which satisfies the condition $\tau_{int} > 3$ in the standard SP RK 2.04-107-2022. At the same time, survey of the internal surface of the upper floor slab showed (Fig. 24) that there are no heat losses through this surface, which can be explained by the selected design solution in the form of a warm attic, discussed in the subsection 3.1.3.

4. CONCLUSIONS

To summarize the results of the thermovision studies for building enclosures, the following conclusions should be made:

1. An analysis of the thermograms of the external end enclosures that correspond to the upper right

corner joint of Room No.1 and the upper left corner joint of Room No.2 shows a significant temperature drop 14.2 - 19.4 °C between the internal surface of external enclosure and internal air temperature of the room, which does not comply with the standard for thermal protection of buildings.

2. An analysis of the thermograms of the internal surfaces of external enclosures that correspond to the upper left corner joint of Room No.1 and the upper right corner joint of Room No.2 showed a temperature drop of 6.4 - 9.0 °C between the internal surface of external enclosures and internal air temperature of the room, which does not comply with the thermal protection standard for buildings as well.

3. An analysis of the thermograms in vulnerable places in the form of window aperture showed that the vertical joints of window apertures of rooms No.1 and No.2 do not comply with the standards, because the temperature value at external wall joint and window frame showed a significant drop to -18 °C and -9.3 °C respectively, where the total area of non-compliance with the standard was over 10%.

4. An analysis of the thermograms in vulnerable areas in the form of window sill joints showed that this area has significant problems as well, because the temperature drops in rooms No.1 and No.2 was -21.1 °C and -9.3 °C, and the total area of vulnerable place was 15.7 % and 6.5 %, respectively.

5. An analysis of the thermograms of external corner, where the reinforced concrete column is located, showed that minimum temperature on the internal surface is 6.5 °C, and the area of the unfavorable zone is 34.8 % of the total, which also contradicts the standard on thermal protection of buildings.

6. An analysis of outdoor and indoor temperatures showed that with temperature drop during the day from -7 °C to -23 °C, the indoor temperature of the room remains relatively stable at the level of 25.3 - 26.1 °C despite the existence of problems with thermal protection of enclosures, which indicates overconsumption of heat energy. At that, the internal air temperature exceeds the permissible temperature for residential premises by 1.3 - 2.6 °C, that contradicts the standards for microclimate parameters. Besides, an analysis of indoor air humidity also showed unsatisfactory values, which during the day varied from 17.4% to 21.2%.

7. An analysis of the thermograms of translucent opening surface and internal surface of the upper floor slab showed satisfying results, with an average surface temperature equals 11.7°C and 23.9°C, respectively, that indicates a correct selection of design solutions in the design, analyzed in subsections 3.1.2 and 3.1.3.

The problems identified by in situ thermovision study indicate that there are problems with the thermal protection of external enclosures. Despite the fact that the object of this study is a new multi-apartment residential building of high comfort in 2020, improvement of external enclosure design currently requires focused attention. In order to achieve more objective results, the problem in improving the comfort in the indoor environment requires additional surveys for different categories (social, municipal, commercial, etc.) of buildings with an aim to develop and improve the design of external enclosures to get optimal values in the issue of improving the energy efficiency of the structural envelope and energy saving of buildings in general, with regard to the climatic characteristics of the northern region of Kazakhstan.

REFERENCES

- [1] Zhangabay N., Abshenov K., Bakhbergen S., Zhakash A., Moldagaliyev A. Evaluating the Effectiveness of Energy-Saving Retrofit Strategies for Residential Buildings. *Int. Rev. Civ. Eng.* 2022. 13. P. 118 – 126. DOI: <https://doi.org/10.15866/irece.v13i2.20933>
- [2] Boronbaev E. Energy Saving Architecture Concept: Buildings with Low Energy Consumption and Emissions in Kyrgyzstan. *E3S Web of Conferences.* 2023. 405. P. 04039 DOI: <https://doi.org/10.1051/e3sconf/202340504039>
- [3] IEA (2020), *Energy Efficiency 2020*, IEA, Paris <https://www.iea.org/reports/energy-efficiency-2020>
- [4] Shandilya A., & Streicher W. Performance and Cost Analysis of Retrofit Strategies Applied to a Sample Single Family House Located in New Delhi India Assisted by TRNSYS Energy Simulation Tool-A Case Study. *International Journal of Engineering and Technical Research.* 2017. 6 (11). P. 304 – 312. DOI: <https://doi.org/10.17577/IJERTV6IS110138>

- [5] Shandilya A., Hauer M., & Streicher W. Optimization of Thermal Behavior and Energy Efficiency of a Residential House Using Energy Retrofitting in Different Climates. 2020, *Civil Engineering and Architecture*. 8 (3). P. 335 – 349. DOI: <https://doi.org/10.13189/cea.2020.080318>
- [6] Dubrakova O.K. Optimization of thermal modernization of a group of buildings using simulation modeling. *Journal of Applied Engineering Science*. 2019. 17 (2). P. 192 – 197. DOI: <https://doi.org/10.5937/jaes17-21683>
- [7] Alsabry A., Truszkiewicz P., Szymański K., Łaskawiec K., & Rojek Ł. Analysis of energy consumption and possibilities of thermal-modernization in residential buildings in Poland case study: the town of Zielona Góra. *International Journal of Applied Mechanics and Engineering*. 2017. 22 (4). DOI: <https://doi.org/10.1515/ijame-2017-0070>
- [8] Sarvajcz-Bánóczy E., Szemes P.T., Husi G. (2018, April). Computer-aided opportunities in modernization of residential buildings. In 2018 2nd International Symposium on Small-scale Intelligent Manufacturing Systems. 2018. P. 1 – 6. DOI: <https://doi.org/10.1109/SIMS.2018.8355292>
- [9] Strelkov Yu.M., Sabitov L.S., Klyuev S.V., Klyuev A.V., Radaykin O.V., Tokareva L.A. Technological features of the construction of a demountable foundation for tower structures. *Construction Materials and Products*. 2022. 5 (3). P. 17 – 26. <https://doi.org/10.58224/2618-7183-2022-5-3-17-26>
- [10] Modernization programs of housing and communal services of the Republic of Kazakhstan for 2011-2020. Resolution of the Government of the Republic of Kazakhstan dated April 30, 2011 473. It became invalid by the Decree of the Government of the Republic of Kazakhstan dated June 28, 2014. 728. <https://adilet.zan.kz/rus/docs/P1100000473>
- [11] Kazakhstan Center for Modernization and Development of Housing and Communal Services <https://zhkh.kz/>
- [12] Ling-Chin, J., Taylor, W., Davidson, P., Reay, D., Tassou, S., & Roskilly, A. P. UK policies and industrial stakeholder perspectives on building thermal performance. *Energy Procedia*. 2019. 158. P. 3375-3380. DOI: <https://doi.org/10.1016/j.egypro.2019.01.948>
- [13] Matic D., Calzada J. R., Eric M., & Babin M. Economically feasible energy refurbishment of prefabricated building in Belgrade, Serbia. *Energy and buildings*. 2015. 98. P. 74 – 81. <https://doi.org/10.1016/j.enbuild.2014.10.041>
- [14] Michalak P. Selected Aspects of Indoor Climate in a Passive Office Building with a Thermally Activated Building System: A Case Study from Poland. *Energies*. 2021. 14 (4). P. 860. DOI: <https://doi.org/10.3390/en14040860>
- [15] Rinquet L., & Schwab. Energetic refurbishment—a global approach for the building envelope. *Energy Procedia*. 2017. 122. P. 109 – 114. DOI: <https://doi.org/10.1016/j.egypro.2017.07.384>
- [16] Nik V. M., Mata E., Kalagasidis A. S., & Scartezzini J. L. Effective and robust energy retrofitting measures for future climatic conditions-Reduced heating demand of Swedish households. *Energy and Buildings*. 2016. 121. P. 176 – 187. DOI: <https://doi.org/10.1016/j.enbuild.2016.03.044>
- [17] Boronbaev E. Energy Saving Architecture: Multidisciplinary Improvement of Buildings Shape, Energy-Efficiency, Microclimate, Seismic-Resistance and Prevention Influences of Thermal Bridges and Mold Growth. In: Jeon, HY. (eds) *Proceedings of the International Conference on Geosynthetics and Environmental Engineering. ICGEE 2023. Lecture Notes in Civil Engineering*. 374. Springer, Singapore. DOI: https://doi.org/10.1007/978-981-99-4229-9_22
- [18] Zhangabay N., Baidilla I., Tagybayev A., Sultan B. Analysis of Thermal Resistance of Developed Energy-Saving External Enclosing Structures with Air Gaps and Horizontal Channels. *Buildings* 2023. 13. P.356. DOI: <https://doi.org/10.3390/buildings13020356>
- [19] Zhangabay N., Bonopera M., Baidilla I., Utelbayeva A., Tursunkululy T. Research of Heat Tolerance and Moisture Conditions of New Worked-Out Face Structures with Complete Gap Spacings. *Buildings* 2023. 13(11). P. 2853. DOI: <https://doi.org/10.3390/buildings13112853>

- [20] Zhangabay N., Baidilla I., Tagybayev A., et al. Thermophysical indicators of elaborated sandwich cladding constructions with heat-reflective coverings and air gaps. *Case Studies in Construction Materials*. 2023. 18. P. e02161. DOI: <https://doi.org/10.1016/j.cscm.2023.e02161>
- [21] Kolesnikov A., Fediuk R., Amran M., Klyuev S., Klyuev A., Volokitina I., Naukenova A., Shapalov Sh., Utelbayeva A., Kolesnikova O., Bazarkhankyzy A. Modeling of Non-Ferrous Metallurgy Waste Disposal with the Production of Iron Silicides and Zinc Distillation. *Materials*. 2022. 15(7). 2542.
- [22] Volokitina I., Kolesnikov A., Fediuk R., Klyuev S., Sabitov L., Volokitin A., Zhuniskaliyev T., Kelamanov B., Yessengaliev D., Yerzhanov A., Kolesnikova, O. Study of the Properties of Antifriction Rings under Severe Plastic Deformation. *Materials*. 2022. 15(7). 2584.
- [23] Zhangabay N., Tagybayev A., Utelbayeva A., et al. Analysis of the influence of thermal insulation material on the thermal resistance of new facade structures with horizontal air channels. *Case Studies in Construction Materials*. 2023. 18. P. e02026. DOI: <https://doi.org/10.1016/j.cscm.2023.e02026>
- [24] Barnshaw S. The zero carbon and nearly zero energy standards in new buildings. *Journal of Building Survey, Appraisal & Valuation*. 2018. 6 (4). P. 344 – 349. DOI: <https://www.ingentaconnect.com/content/hsp/jbsav>
- [25] Klyuev S.V., Kashapov N.F., Radaykin O.V., Sabitov L.S., Klyuev A.V., Shchekina N.A. Reliability coefficient for fibreconcrete material. *Construction Materials and Products*. 2022. 5 (2). P. 51 – 58. <https://doi.org/10.58224/2618-7183-2022-5-2-51-58>
- [26] Maurício M., Enrico B., Letícia A., Yuri de S., Almeida E., Renan P. Infrared thermal imaging to inspect pathologies on façades of historical buildings: A case study on the Municipal Market of São Paulo, Brazil. *Case Studies in Construction Materials*. 2022. 16. P. e01122. DOI: <https://doi.org/10.1016/j.cscm.2022.e01122>
- [27] Letzai Ruiz Valero, Virginia Flores Sasso, Esteban Prieto Vicioso. In situ assessment of superficial moisture condition in façades of historic building using non-destructive techniques. *Case Studies in Construction Materials*. 2019. 10. P. e00228. DOI: <https://doi.org/10.1016/j.cscm.2019.e00228>

INFORMATION ABOUT THE AUTHORS

Zhangabay N., e-mail: Nurlan.Zhanabay777@mail.ru, tel.: +7-702-432-72-21, ORCID: <https://orcid.org/0000-0002-8153-1449>, SCOPUS: <https://www.scopus.com/authid/detail.uri?authorId=57211557292>, South-Kazakhstan University named after M. Auezov, Department «Architecture and urban planning», Candidate of Engineering sciences (PhD), Associate Professor

Giyasov A., e-mail: adham52@mail.ru, tel.: +7-985-481-80-33, ORCID: <https://orcid.org/0000-0002-5982-8983>, SCOPUS: <https://www.scopus.com/authid/detail.uri?authorId=57202817395>, Moscow State University of Civil Engineering (MGSU), Department of Architectural and Construction Design and Environmental Physics, Doctor of Engineering sciences, Professor

Ybray S., e-mail: sultanybray@gmail.com, tel.: +7-707-705-75-79, ORCID: <https://orcid.org/0000-0002-5262-2149>, SCOPUS: <https://www.scopus.com/authid/detail.uri?authorId=57202946965>, Kazakh Agrotechnical Research University named after S. Seifullin, Department of Heat Power Engineering, Doctoral student

Tursunkululy T., e-mail: timurtursunkululy@gmail.com, tel.: +7-705-557-77-22, ORCID: <https://orcid.org/0000-0001-6215-7677>, SCOPUS: <https://www.scopus.com/authid/detail.uri?authorId=57687675500>, South-Kazakhstan University named after M. Auezov, Department «Architecture and urban planning», PhD

Kolesnikov A., e-mail: kas164@yandex.kz, tel.: +7-705-256-68-97, ORCID: <https://orcid.org/0000-0002-8060-6234>, SCOPUS: <https://www.scopus.com/authid/detail.uri?authorId=57189499212>, South-Kazakhstan University named after M. Auezov, Department of Life safety and environmental protection, Candidate of Engineering sciences (PhD), Associate Professor